Available online at www.sciencedirect.com
ScienceDirect
Catalysis Today 118 (2006) 279–287
CATALYSIS TODAY
www.elsevier.com/locate/cattod

Oxidative dehydrogenation of ethane to ethylene over alumina-supported vanadium oxide catalysts: Relationship between molecular structures and chemical reactivity

M.V. Martínez-Huerta [a], X. Gao [b], H. Tian [b], I.E. Wachs [b], J.L.G. Fierro [c], M.A. Bañares [c,*]

[a] *Departamento de Química Física, Universidad de La Laguna, C/Astrofísico Francisco Sánchez s/n, E-38071, La Laguna, Tenerife, Spain*
[b] *Operando Molecular Spectroscopy & Catalysis Laboratory, Department of Chemical Engineering, Lehigh University, Bethlehem, PA 18015, USA*
[c] *Departamento de Estructura y Reactividad, Instituto de Catálisis y Petroleoquímica, CSIC, Marie Curie, 2, E-28049 Madrid, Spain*

Available online 22 August 2006

Abstract

The influence of vanadium oxide loading in the supported VO_x/Al_2O_3 catalyst system upon the dehydrated surface vanadia molecular structure, surface acidic properties, reduction characteristics and the catalytic oxidative dehydrogenation (ODH) of ethane to ethylene was investigated. Characterization of the supported VO_x/Al_2O_3 catalysts by XPS surface analysis and Raman spectroscopy revealed that vanadia was highly dispersed on the Al_2O_3 support as a two-dimensional surface VO_x overlayer with monolayer surface coverage corresponding to ~9 V/nm^2. Furthermore, Raman revealed that the extent of polymerization of surface VO_x species increases with surface vanadia coverage in the sub-monolayer region. Pyridine chemisorption-IR studies revealed that the number of surface Brønsted acid sites increases with increasing surface VO_x coverage and parallels the extent of polymerization in the sub-monolayer region. The reducibility of the surface VO_x species was monitored by both H_2-TPR and in situ Raman spectroscopy and also revealed that the reducibility of the surface VO_x species increases with surface VO_x coverage and parallels the extent of polymerization in the sub-monolayer region. The fraction of monomeric and polymeric surface VO_x species has been quantitatively calculated by a novel UV–Vis DRS method. The overall ethane ODH TOF value, however, is constant with surface vanadia coverage in the sub-monolayer region. The constant ethane TOF reveals that both isolated and polymeric surface VO_x species possess essentially the same TOF value for ethane activation. The reducibility and Brønsted acidity of the surface VO_x species, however, do affect the ethylene selectivity. The highest selectivity to ethylene was obtained at a surface vanadia density of ~2.2 V/nm^2, which corresponds to a little more than ~0.25 monolayer coverage. Below 2.2 V/nm^2, exposed Al support cations are responsible for converting ethylene to CO. Above 2.2 V/nm^2, the enhanced reducibility and surface Brønsted acidity appear to decrease the ethylene selectivity, which may also be due to higher conversion levels. Above monolayer coverage, crystalline V_2O_5 nanoparticles are also present and do not contribute to ethane activation, but are responsible for unselective conversion of ethylene to CO. The crystalline V_2O_5 nanoparticles also react with the Al_2O_3 support at elevated temperatures via a solid-state reaction to form crystalline $AlVO_4$, which suppresses ethylene combustion of the crystalline V_2O_5 nanoparticles. The molecular structure–chemical characteristics of the surface VO_x species demonstrate that neither the terminal V=O nor bridging V–O–V bonds influence the chemical properties of the supported VO_x/Al_2O_3 catalysts, and that the bridging V–O–Al bond represents the catalytic active site for ethane activation.

Keywords: Catalyst; Supported; Alumina; Vanadium oxide; H_2-TPR; TPR-Raman; TPO-Raman; Oxidative dehydrogenation; ODH; Ethane; Ethylene; Raman; IR; In situ; Pyridine; Acid sites; Surface; Lewis; Brønsted

1. Introduction

Ethane is the second major component of natural gas, which makes it a potential source for ethylene, which is commonly used for the production of low density polyethylene, high density polyethylene, ethylene oxide, as well as many other

* Corresponding author. Tel.: +34 91 585 4788; fax: +34 91 585 4760.
E-mail address: banares@icp.csic.es (M.A. Bañares).

0920-5861/$ – see front matter © 2006 Elsevier B.V. All rights reserved.
doi:10.1016/j.cattod.2006.07.034

compounds made from C_2 hydrocarbons. Despite this potential source of ethylene, no industrial process currently operates for the conversion of ethane to ethylene [1], but important progress is being made [2]. Oxidative dehydrogenation (ODH) of light alkanes is an energetically efficient process, because the presence of oxygen lowers the thermodynamic restrictions for dehydrogenation [3]. However, the yield to alkenes on most of the catalysts used is not satisfactory, due to the side reactions leading to the formation of CO_x. Thus, understanding of the parameters that make the catalysts efficient for the heterogeneous catalysis for the oxidative dehydrogenation of ethane is currently very important.

Vanadium-based catalysts are among the most active and selective for ODH of light alkanes. The redox properties of the catalyst are important for reactions which proceed via the Mars-van-Krevelen mechanism. Hydrocarbon molecules react with oxygen associated with the vanadia and the reduced vanadium cations are reoxidized by gas phase molecular O_2. The average oxidation state during catalytic operation depends on the relative rates of reduction and reoxidation, which for alkane oxidation over supported vanadium oxide catalysts appears to leave the supported oxide essentially oxidized [4].

The molecular structure of the supported VO_x species has been clearly revealed by the application of several ground breaking in situ spectroscopic investigations during the 1980s [5]. The dehydrated surface VO_x species are usually exclusively present as isolated surface $(–Support–O)_3–V{=}O$ species at low surface VO_x coverage and the extent of polymerization increases with surface VO_x coverage, which has only one V–O–support bond per vanadium atom and two being bridging V–O–V bonds. A quantitative method, based on UV–vis diffuse reflectance spectroscopy (DRS), has recently been developed to determine the fraction of monomeric and polymeric surface VO_x species present in supported VO_x on silica, alumina and zirconia [6]. This method is also employed in the present investigation of alumina-supported vanadia catalysts.

The activity of supported vanadia catalysts is strongly affected by the interaction with the specific oxide support and texture [1,7]. Alumina supports constitute a family of materials whose importance in the field of heterogeneous catalysis is significant [8]. The solid-state chemistry of aluminum oxides is very complex with several different meta-stable crystal phases forming under different synthesis conditions, and also may involve the cations supported on them (e.g., Mo [9], V [10,11] or Sb [12]). One of the most important features of alumina supports is their surface acidity, and IR spectroscopy coupled with chemisorption of basic chemical probe molecules has been used extensively for determination of acidity [13]. The best results in the determination of the total acidity of alumina supports can be obtained by the adsorption–desorption of pyridine (Py) [14]. In fact Py, although less basic than ammonia, is a fairly hard base that interacts with widely different surface acid sites.

The interaction of the surface vanadia species and the oxide support has a profound effect on the catalytic properties of the supported vanadium oxide catalysts. However, there is no clear relationship between the structure of surface vanadia species and their reactivity for the ODH of lower alkanes. The objective of this study is to evaluate the effect of vanadium oxide loading on Al_2O_3 for ethane ODH to ethylene and relate its catalytic performance to changes in surface vanadia molecular structure, surface redox and surface acidic characteristics.

2. Experimental

Vanadium oxide was supported on γ-alumina by the incipient wetness impregnation technique [15] to obtain catalyst loading ranging from 1 to 30 wt.% of V_2O_5 on Al_2O_3. The catalysts are referred to as "*x*VAl", where "*x*" represents the weight percent of V_2O_5 on Al_2O_3. The fraction of polymerized surface vanadium oxide species was determined based on the methodology described elsewhere [6]. Surface vanadium loading (V at/nm^2) was calculated with respect to the BET area of the alumina support.

The BET surface areas of the samples were determined by N_2 adsorption at −196 °C in a Micromeritics system Model 2000 ASAP. The composition of the near-surface region (sampling depth of 3–5 nm) of the supported V_2O_5/Al_2O_3 catalysts was investigated using X-ray photoelectron spectroscopy (XPS). The XPS analysis was performed in a Fisons ESCALAB 200R electron spectrometer equipped with a hemispherical electron analyzer and a Mg Kα X-ray source ($h\nu$ = 1253.6 eV) powered at 120 W. A PDP 11/05 computer from DEC was used for collecting and analyzing the spectra. The samples were placed in small copper cylinders and mounted in a transfer rod placed in the pretreatment chamber of the instrument. The base pressure in the ion-pumped analysis chamber was maintained below 5×10^{-9} Torr during data acquisition. The XPS signals were collected for 30–100 min with pass energy of 10 eV, which is typical for collection of high resolution spectra.

The in situ Raman spectra were collected with a Renishaw Micro-Raman System 1000 equipped with a cooled CCD detector (−73 °C) and a holographic super-Notch filter that removes the elastic laser scattering. The samples were excited with the 514.5 nm Ar+ line. An in situ environmental cell (Linkam, TS-1500) allowed control of catalyst temperature, gas composition and flow rates. The samples were maintained in powder form to minimize mass transfer limitations and ensure that all catalytic material in the cell is exposed to the flowing gases. The spectral resolution is ∼3 cm^{-1} and the spectral acquisition consisted of five 60 s accumulations (300 s) for each sample. The samples for the in situ measurements were initially pretreated in O_2/He at 450 °C for 4 h prior to any other treatments. The Raman spectra of dehydrated samples were run at 150 °C, after the pretreatment at 450 °C. The temperature-programmed (TP)-Raman studies, TPO- and TPR-Raman, were performed by heating the catalyst sample stepwise in synthetic air or 10% H_2/Ar, respectively [16]. Although Raman spectroscopy penetrates ca. ∼1 μm in the catalyst, it provides the molecular structures of both surface and bulk phases, particularly for supported oxide, where the supported component is initially located at the surface [15]. The reaction in situ Raman spectra under ethane ODH (C_2H_6/O_2/He molar

ratio = 1/2/8) and DH (C_2H_6/He molar ratio = 1/8)) reaction conditions were performed using the same reaction feed as in the catalytic runs, further information can be found elsewhere [15,17,18].

The in situ UV–vis DRS spectra were obtained with a Varian Cary 5E UV–vis spectrophotometer employing the integration sphere diffuse reflectance attachment, and an in situ cell (Harrick, HVC-DR2) as described elsewhere [6]. The UV–vis DRS spectra of the bulk vanadate reference compounds were obtained under ambient conditions, and the spectra of the dehydrated supported vanadia catalysts were obtained after the samples were treated at 400 °C in flowing 10% O_2/He gas (30 mL/min) for 1 h to desorb the adsorbed ambient moisture. The Kubelka–Munk function $F(R_\infty)$ was extracted from the UV–vis DRS absorbance and the edge energy (Eg) for allowed transitions was determined by finding the intercept of the straight line in the low-energy rise of the plot of $[F(R_\infty)h\nu]^2$ against $h\nu$, where $h\nu$ is the incident photon energy [6].

The H_2 temperature programmed reduction (H_2-TPR) experiments were run in a Micrometrics equipment model TPR/TPD-2900 fitted with a TCD detector. Samples of ca. 20 mg each were used. The TPR experiments were run in a 10% H_2/Ar stream, with a heating rate of 10 °C/min and 80 cm^3/min flow rate.

FTIR spectra were collected with a Nicolet equipment model 5ZDX fitted with a DTGS detector. The spectral resolution is ~4 cm^{-1} and the spectral acquisition consisted of 100 accumulations for each spectrum. Spectra of KBr were subtracted from all spectra. Pyridine adsorption was made at room temperature.

Ethane oxidation was carried out in an isothermal fixed-bed down-flow reactor containing 20 mg of the catalyst. The reaction was evaluated in the temperature range of 450–610 °C at atmospheric pressure. The reaction gas mixture consisted of C_2H_6/O_2/He (molar ratio = 1/2/8) with a total flow rate of 30 cm^3/min. The TOF values were calculated assuming that all the vanadia is dispersed, which was confirmed by Raman spectroscopy. Conversion is defined as the fraction of the ethane reactant converted to reaction products, selectivity is defined as fraction of reaction products that form ethylene, and the yield is defined as the total amount of ethylene produced (conversion × selectivity).

Table 1

Catalysts	Abs. Atom. $\%V_2O_5/Al_2O_3$	BET (m^2/g)	Atom. ratio V/Al-XPS	V/nm^{2a}	atV/g
Al_2O_3	0	222	0	0	0
1VAl	1.4	221	0.002	0.4	9.0×10^{22}
3VAl	4.2	219	0.007	1.3	2.8×10^{23}
5VAl	6.9	217	0.014	2.2	4.6×10^{23}
10VAl	14.1	217	0.047	4.9	9.3×10^{23}
15VAl	18.9	207	0.060	7.0	1.3×10^{24}
20VAl	24.9	173	0.074	9.9	1.7×10^{24}
25VAl	31.0	165	0.082	13.4	2.1×10^{24}
30VAl	39.4	171	0.079	19.4	2.7×10^{24}

[a] Referred to the BET area of alumina support (222 m^2/g).

3. Results

3.1. Characterization of fresh catalysts

The physicochemical characteristics of the catalysts are listed in Table 1. From the table, it is observed that the BET surface area decreases with an increase in vanadium oxide loading, which is primarily due to the added mass of the vanadia. The XPS V/Al atomic ratio also increases linearly with vanadium oxide loading up to 20VAl, then levels off. This suggests a high dispersion degree of vanadium oxide species up to a loading between 15VAl and 20VAl (i.e., between 7 and 10 V atoms/nm^2), which corresponds to monolayer surface coverage.

3.1.1. In situ Raman spectroscopy studies

The in situ Raman spectra of 0–30% VO_x/Al_2O_3 under dehydrated conditions (450 °C) are presented in Fig. 1. The Al_2O_3 support does not exhibit Raman bands due to the ionic character of the Al–O bond. Crystalline V_2O_5 vibrations at 141, 191, 281, 406, 526, 695 and 993 cm^{-1} are not present at the lower vanadia loadings and are only present above monolayer surface vanadia covearge, which corresponds to ~9 V/nm^2 and is in agreement with the XPS results. The vibration at ~1010 cm^{-1} arises from the

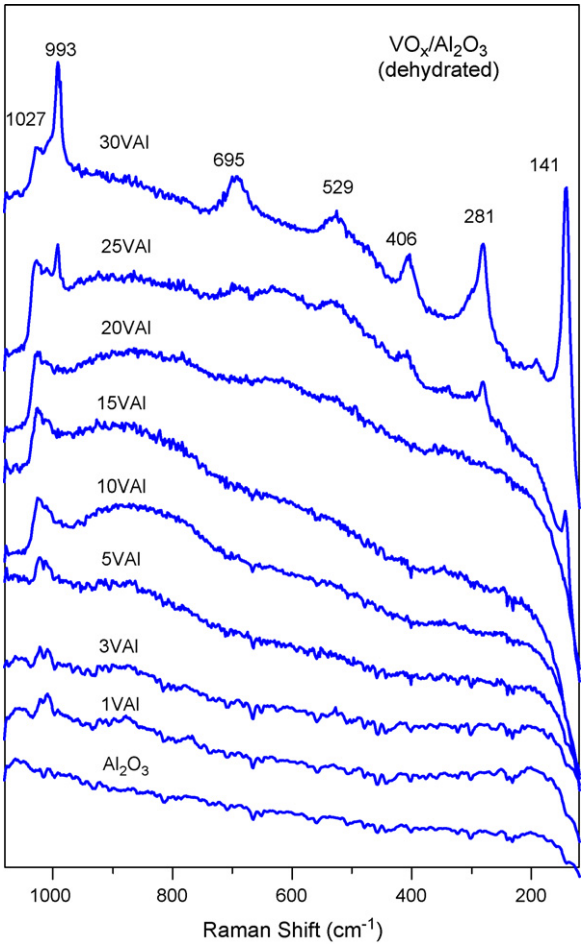

Fig. 1. The in situ Raman spectra of 0–30% VO_x/Al_2O_3 under dehydrated conditions (450 °C).

terminal V=O bond of isolated surface vanadia species $(Al\text{-}O)_3$-V=O [19], and is the predominant Raman band at low vanadium loading (until ~5VAl). As vanadia loading increases, the terminal V=O vibration shifts to higher frequencies and a broad feature at ~860 cm^{-1}also becomes apparent, which has previously been assigned to the vibration of the bridging V–O–Al bond [20]. The Raman band at ~340 cm^{-1} is characteristic of the bending mode of the dehydrated surface VO_x species [21]. In addition, new Raman bands are also present at ~620 and ~780 cm^{-1} for high vanadia loaded samples that arise from the symmetric and asymmetric stretching modes of the bridging V–O–V functionality of the polymeric surface vanadia species. The increase of polymeric surface vanadia species with vanadia loading, suggests that Raman band at 1010 cm^{-1} correspond to V=O functionality of isolated surface vanadia species and 1023 cm^{-1} to V=O functionality of polymeric surface vanadia species.

3.1.2. *In situ oxidizing environments*

The dehydrated 25VAl catalyst was heated stepwise in the in situ Linkam cell in dry air stream. Fig. 2 shows representative Raman spectra. Alumina-supported vanadium oxide catalyst containing the crystalline V_2O_5 nanoparticles undergo solid-state reaction to form bulk $AlVO_4$ (281, 322, 397, 463, 514, 557, 851, 900, 918, 947, 984 and 1012 cm^{-1}) [10,11,22] above 570 °C.

3.1.3. *In situ hydrocarbon reducing environments*

Similarly, the dehydrated catalysts were heated stepwise in the in situ cell in the reducing reactive environment of C_2H_6/He. The in situ TPR-Raman spectra of 15% V_2O_5/Al_2O_3 are shown in Fig. 3. The Raman bands at 895 cm^{-1} (V–O–Al) and 1029 cm^{-1} (V=O) significantly decrease with temperature as the extent of reduction of the surface vanadia species progresses.

The H_2-TPR profiles of the supported VO_x/Al_2O_3 catalysts are presented in Fig. 4. The supported 1VAl catalyst exhibits one reduction peak at 550 °C, which shifts progressively to lower values with increasing vanadia coverage up to 15VAl (466 °C). This band then shifts progressively to higher peak temperatures, 503 °C for 30VAl, with increasing vanadia loading above monolayer surface coverage.

The total number and distribution of surface Lewis and Brønsted acid sites of the supported VO_x/Al_2O_3 catalysts were determined by the adsorption–desorption of pyridine. The FT-IR spectra of pyridine adsorbed at room temperature and after evacuation at 120 °C are presented in Fig. 5. The surface Lewis

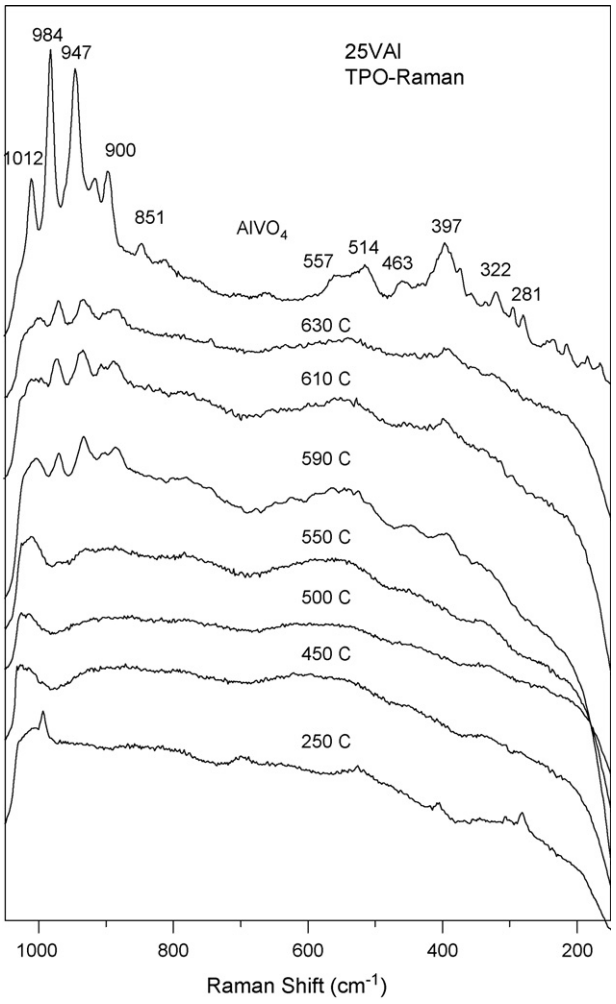

Fig. 2. Representative in situ *TPO*-Raman spectra of 25VAl. $AlVO_4$ is included for reference on top of all spectra.

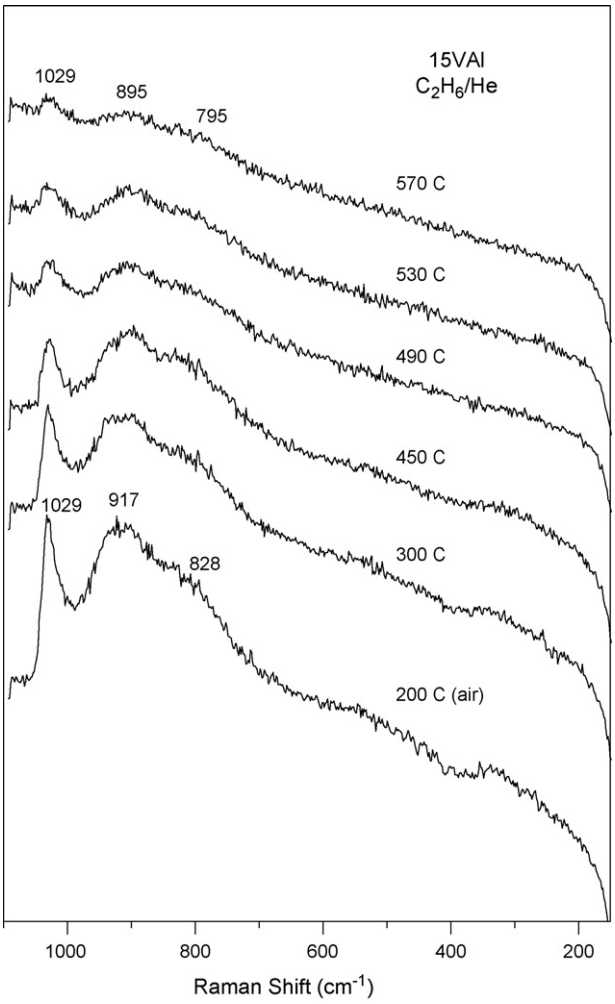

Fig. 3. Representative in situ TPR-Raman under C_2H_6/He of 15VAl.

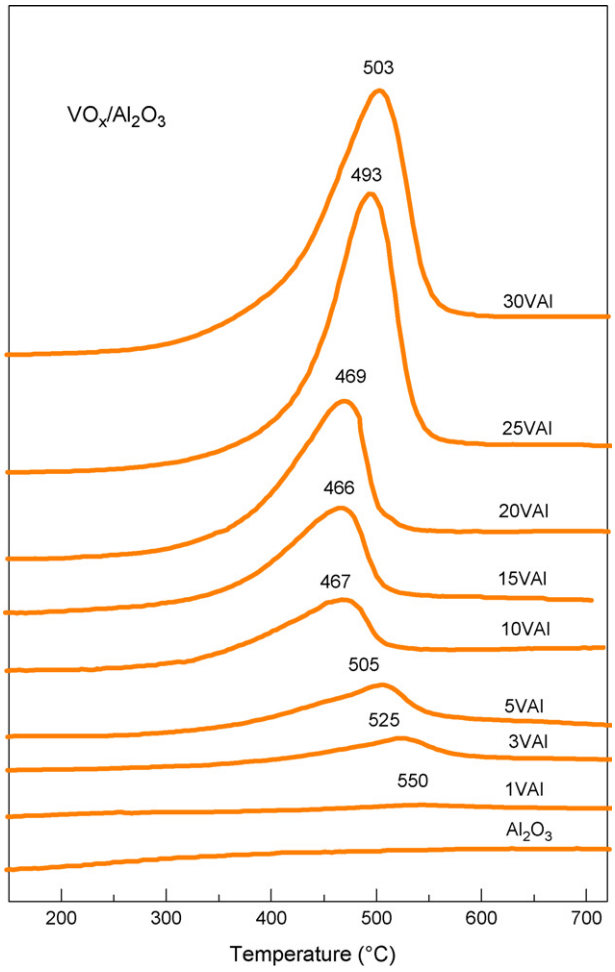

Fig. 4. H2-TPR profile of VO_x/Al_2O_3 catalysts.

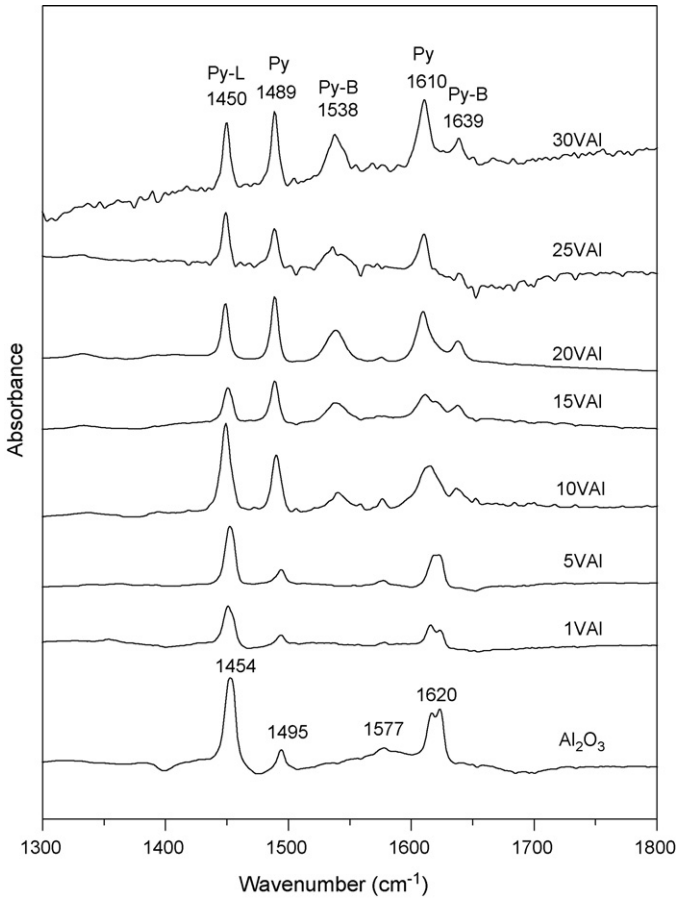

Fig. 5. FTIR spectra using pyridine adsorption.

acid sites (LAS) exhibit IR bands at 1450 and 1578 cm^{-1} and the surface Brønsted acid sites (BAS) vibrations occur at 1450 and 1638 cm^{-1}. The alumina support only possess surface LAS and surface BAS start to appear at 3 V/nm^2 and higher loadings. Vanadia species must titrate the alumina LAS.

The relationship between ratio of number of surface Brønsted acid sites (NBAS) (1538 cm^{-1}) and number of surface Lewis acid sites (NLAS) (1450 cm^{-1}) (NBAS/NLAS) versus vanadia loading is plotted in Fig. 6 along with the reducibility data and degree of polymerization of the surface VO_x species [6]. The number of the surface Lewis acid sites of the VO_x/Al_2O_3 catalysts decreases with V_2O_5 loading suggesting that they mainly originate from exposed alumina sites. No surface Brønsted acid sites are detected up to approximately half a monolayer of surface vanadia species on alumina and further increase with increasing surface vanadia coverage. The number of surface Brønsted acid sites reaches a maximum at ~20 wt.% of V_2O_5 (9.9 V at/nm^2) corresponding to monolayer coverage. Above monolayer surface vanadia coverage, the number of surface BAS slightly decreases when the crystalline V_2O_5 nanoparticles are present on top of the surface VO_x monolayer and cover some of the surface vanadia species. Similar trends were also reported by Akbas et al. [23]. Increasing the surface vanadia coverage in the sub-monolayer region also promotes the reducibility of supported VO_x species up to ca. 9.9 V at/nm^2. It is interesting to observe that both trends parallel the continuous increase in the polymerization degree of the surface vanadia species as shown in Fig. 6 [6].

3.2. Oxidative dehydrogenation of ethane

The ethane ODH catalytic performance data are listed in Table 2 for reaction temperatures of 470, 510 and 550 °C. As expected, ethane conversion increases with reaction temperature since the Arrhenius rate increases with temperature. Ethane conversion initially increases with vanadia loading up to 20VAl (9 V/nm^2), and then decreases with additional vanadia loading. At low vanadia loading, the selectivity towards CO and CO_2 are high. With increasing surface vanadia loading, the CO_2 selectivity decreases and the CO selectivity passes through a minimum at 5VAl (2.25 V/nm^2). The ethylene selectivity varies inversely to that of the CO selectivity, reaching its maximum selectivity at 5VAl (2.25 V/nm^2).

The product yields are illustrated in Fig. 7. Pure alumina is not selective and essentially yields CO and CO_2. Addition of vanadia increases ethane conversion and formation of the selective ethylene product. The selectivity trends commented above and the continuous increase in the conversion values result in maximum yield to ethylene for 10–20% VO_x/Al_2O_3

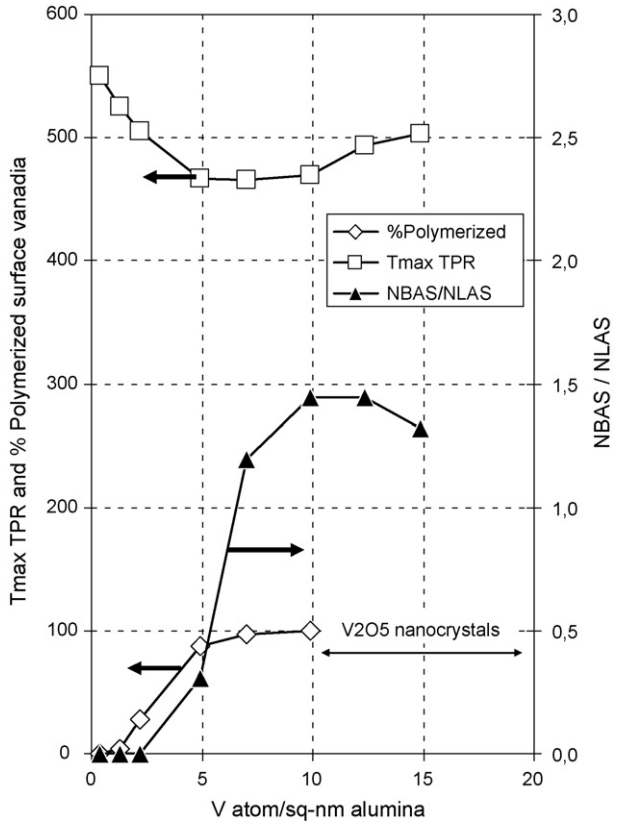

Fig. 6. Reducibility, extent of polymerization and NBAS/NLAS ratio vs. surface vanadium density.

(4.5–9 V/nm^2) catalysts. In this loading range, ethylene production is essentially constant, but CO production increases.

In order to assess the activity per vanadium site and to better understand ethane ODH conversion over the alumina-supported vanadia catalysts, the specific TOF values to ethylene, CO and CO_2 at 470 °C are shown in Fig. 8A. The TOF values to CO increase at loading above monolayer surface vanadia coverage, which coincides with the appearance of crystalline V_2O_5 nanoparticles. In general, the TOF for ethylene passes through a maximum and that for CO, through a minimum with surface vanadia coverage in the sub-monolayer region. In summary, the overall ethane consumption TOF does not change significantly with surface vanadia coverage, but the selectivity to the different products is strongly affected by surface vanadia coverage. The increase in selectivity with initial coverage of vanadia must be due to the titration of non-selective exposed alumina sites. At higher surface vanadia coverage, conversion of ethane increase and secondary reactions of ethylene are enhanced.

The number of surface vanadium sites involved in the rate-determining-step (rds) of ethane ODH to ethylene can be determined by the simplified rate equation

$$r\left[\frac{\text{moles}}{g \times s}\right] = k' P_{C_2} V^n$$

$$k' = k_{RDS} \times K_{ADS}$$

where V represents the vanadia atoms per gram of catalyst, k_{RDS} is the kinetic rate constant of the rate-determining-step (rds),

Table 2
The ethane ODH catalytic performance data of VO_x/Al_2O_3 catalysts for 470, 510 and 550 °C

Catalyst	T (°C)	Conversion (%)	Selectivity (%)		
			C_2H_4	CO_2	CO
Al_2O_3	470	2.0	8	38	55
1VAl		0.6	24	26	51
3VAl		1.2	62	8	31
5VAl		1.9	79	3	21
10VAl		5.8	71	6	20
15VAl		6.9	69	2	29
20VAl		8.0	60	5	35
25VAl		12.1	41	6	53
30VAl		11.6	49	5	46
Al_2O_3	510	5.7	7	34	59
1VAl		1.6	27	22	51
3VAl		2.7	60	8	32
5VAl		3.7	72	4	24
10VAl		12.0	68	6	25
15VAl		13.6	56	5	39
20VAl		18.5	45	5	49
25VAl		23.2	30	8	62
30VAl		22.8	37	6	57
Al_2O_3	550	13.7	6	33	60
1VAl		5.2	27	21	52
3VAl		6.9	59	7	34
5VAl		9.2	70	4	26
10VAl		30.7	57	8	35
15VAl		32.8	40	5	55
20VAl		40.6	26	9	65
25VAl		35.7	23	11	67
30VAl		34.3	27	9	64

K_{ADS} is the ethane equilibrium adsorption constant, P_{C_2} is the partial pressure of ethane (mol^{-1}), and "n" represents the number of surface VO_4 species or catalytic active sites involved in the ethane ODH rate-determining-step. At constant temperature and ethane partial pressure, the value of "n" can be determined directly from the slope of the plot of log r versus log V as the surface vanadia coverage is varied in the

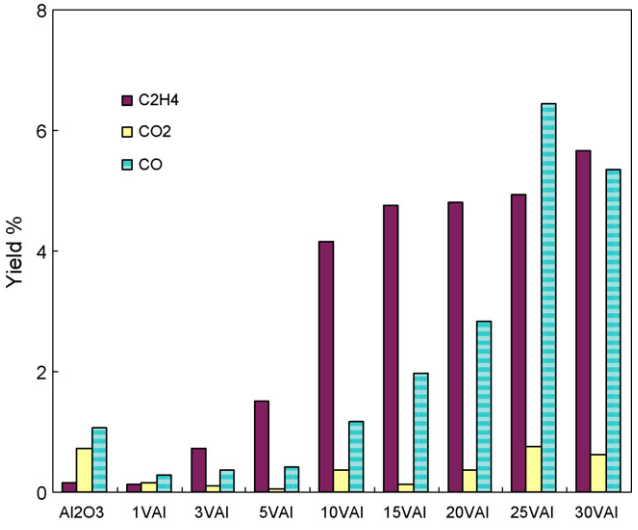

Fig. 7. Yield of C_2H_4, CO_2 and CO at 470 °C of VO_x/Al_2O_3 catalysts.

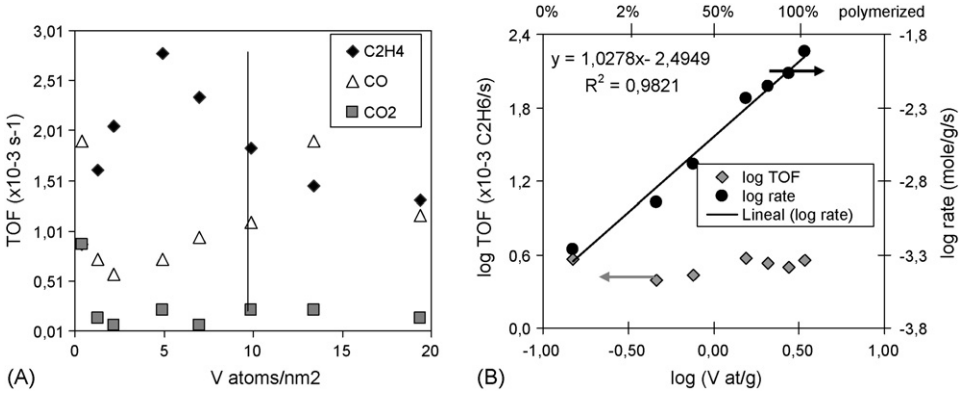

Fig. 8. TOF to ethylene, CO_2 and CO at 470 °C.

sub-monolayer region where vanadia is 100% dispersed as surface vanadia species on the Al_2O_3 support. Fig. 8B illustrates such a kinetic plot, the ethane ODH TOF values, and the polymerization degree of surface vanadia species. The ethane ODH TOF values are not affected by vanadia coverage (i.e., polymerization degree). The plot of the rate yields a slope of ~1, which indicates that only one surface VO_4 site is involved in the rds for ethane ODH to ethylene.

During the ethane ODH reaction, most of the supported VO_x/Al_2O_3 catalysts are stable during time on stream. However, catalysts with 10–30% VO_x/Al_2O_3 (4.5–13.5 V/nm^2) do experience deactivation with time on stream, and the extent of deactivation increases with additional vanadia in this region. Fig. 9 illustrates the yield values of 25VAl (11.25 V/nm^2) versus time on stream at different reaction temperatures. The CO and CO_2 yield values decrease with reaction time at a given temperature, but the ethylene yield values do not change. The extent of deactivation increases with increasing reaction temperature.

3.3. Characterization of used catalysts

In order to fundamentally understand the deactivation process on a molecular level, Raman spectra of dehydrated spent catalysts were examined (see Fig. 10). The temperature was never above 570 °C. No significant structural changes are evident up to 20VAl (9 V/nm^2), but significant structural differences are apparent for loadings above 20VAl (9 V/nm^2). New Raman bands are present in the used 25VAl (11.25 V/nm^2) and 30VAl (13.5 V/nm^2) catalysts. These new and intense bands reflect the formation of crystalline $AlVO_4$, which is included in the figure for reference purposes (Fig. 10). These results underline that the solid-state reaction between the alumina support and supported vanadia to form crystalline $AlVO_4$ under ethane ODH reaction conditions, and may be related to the observed catalyst deactivation.

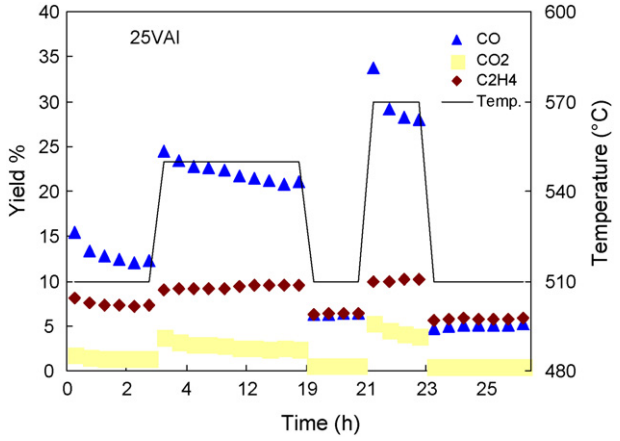

Fig. 9. Yields of CO, CO_2 and C_2H_4 vs. time as function of temperature for 25VAl catalyst.

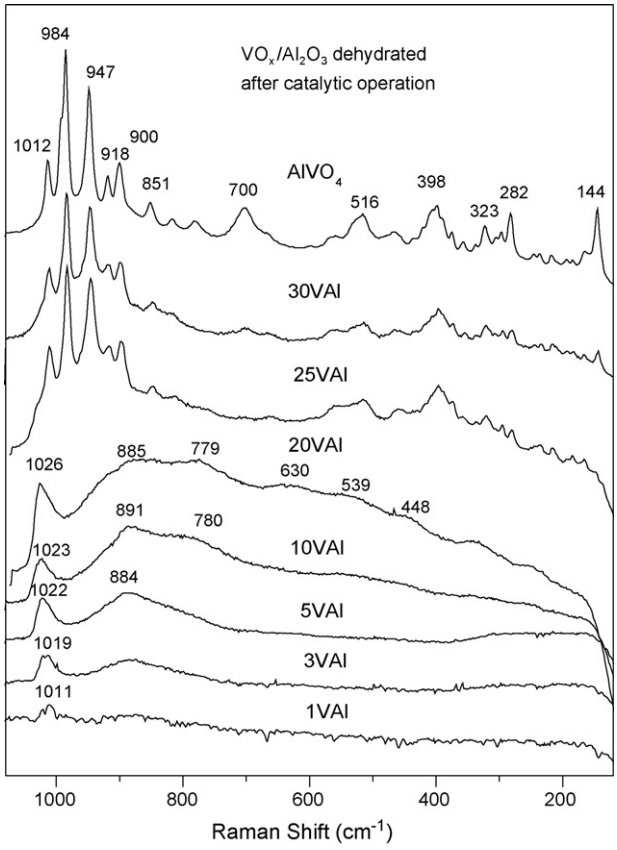

Fig. 10. Raman spectra of dehydrated spent VO_x/Al_2O_3 catalysts after catalytic operation.

4. Discussion

Alumina-supported vanadium oxide catalysts possess dispersed surface vanadium oxide species up to ~9 V/nm^2, which corresponds to monolayer surface vanadia coverage on the alumina support. The analytical results from both XPS surface analysis of the V/Al atomic ratio and the absence of Raman vibrations for crystalline V_2O_5 particles indicate that monolayer surface vanadia coverage corresponds to ~9 V/nm^2. As the vanadia coverage increases in the sub-monolayer region (<9 V/nm^2), the surface vanadia species begin to polymerize and the extent of polymerization increases with coverage [6]. Above monolayer surface vanadia coverage, three-dimensional crystalline V_2O_5 nanoparticles also form on top of the two-dimensional surface vanadia monolayer.

As the surface vanadia coverage increases in the sub-monolayer region, several simultaneous trends take place with the surface VO_x species: formation of dehydrated polymeric species, increased reducibility and increase in Brønsted acidity. The extent of polymerization of the surface vanadia species increases with increasing surface vanadia coverage. The extent of polymerization can be quantitatively determined by UV–vis diffuse reflectance spectroscopy as has recently been reported [6]. The reducibility of the surface vanadia species increases as reflected in the lower H_2-TPR temperatures with increasing surface vanadia coverage. Almost all of the surface vanadia species become polymerized at 15VAl (7 V/nm^2), which corresponds to the most reducible catalyst (see Fig. 8). The overall reducibility of the supported VO_x/Al_2O_3 catalysts decreases above 20VAl (9 V/nm^2) because of the presence of the crystalline V_2O_5 nanoparticles above monolayer coverage. Raman directly confirmed the presence of the V_2O_5 nanoparticles for 25VAl (11.25 V/nm^2) and 30VAl (13.5 V/nm^2). Thus, the H_2 reducibility of the different supported vanadia species follows the trend: polymeric surface VO_x > isolated surface VO_x > crystalline V_2O_5 nanoparticles. It is important to emphasize that the terminal V=O bond of surface vanadia species become stronger with coverage, shifts from 1010 to 1023 cm^{-1}, while the surface vanadia species become increasingly reducible. Thus, the terminal V=O bond must not be involved in the rate-determining-step of H_2 reduction of the surface vanadia species.

The bare alumina support only possesses surface Lewis acid sites with the pyridine chemical probe molecule. The deposition of the surface vanadia species to the alumina support progressively titrate the alumina surface Lewis acid sites. At low surface vanadia coverage, surface Brønsted acid sites are not detected with pyridine. As the surface vanadia species become increasingly polymerized, the surface Brønsted acid sites start to appear. The increase in extent of polymerization of the surface vanadia species parallels the growth of surface Brønsted acid sites with surface vanadia coverage. It, thus, appears that the surface Brønsted acid sites are also associated with the polymeric surface vanadium oxide species on the Al_2O_3 support. In summary, the acid-base and redox properties of the surface vanadia species on Al_2O_3 in the sub-monolayer region are strongly influenced by the extent of polymerization.

The ethane ODH activity data exhibits a continuous increase in ethane conversion with vanadia loading that reaches a plateau or slight maximum at ~25VAl (11.25 V/nm^2). Higher vanadia loading slightly decreases the overall activity indicating that the crystalline V_2O_5 nanoparticles are less active for ethane activation than the surface vanadia species on the alumina support. Note also that the unselective CO_x formation by the alumina support sites is progressively suppressed with increasing vanadia loading. Normalizing the catalytic activity per vanadium site (i.e., TOF number) allows the determination of the relative contributions of the isolated and polymeric surface VO_x species for ethane activation. The essentially constant ethane conversion TOF with surface vanadia coverage in the sub-monolayer region demonstrates that the rates of ethane activation by the isolated and polymeric surface vanadia species are essentially indistinguishable. In addition, the kinetic plot of log rate *vs*. log V also demonstrates that *only one surface VO_4 site is involved in the rds for ethane ODH activation* (Fig. 8B). Thus, the activation of ethane is a structure-insensitive reaction over supported V_2O_5/Al_2O_3 catalysts since this reaction does not require an ensemble of surface VO_x catalytic active sites. Similar trends are demonstrated for propane oxidative dehydrogenation reaction [6]. This effect depends on the specific substrate, for instance, butane oxidation to maleic anhydride does require an ensemble to surface VO_x active sites to produce maleic anhydride efficiently; in such case, activity increases dramatically with coverage [24].

Crystalline $AlVO_4$ particles form at elevated temperature in the presence of the crystalline V_2O_5 nanoparticles above monolayer surface vanadia coverage (see Fig. 2). In general, crystalline $AlVO_4$ is observed at high vanadia loading on alumina support, particularly upon reducing conditions [10]. TPO shows incipient formation of AlVO4 at 630 °C, however, ethane ODH reaction affords significant formation of AlVO4 at 570 °C. The formation of $AlVO_4$ is further accelerated in the ethane ODH reaction environment and its appearance parallels deactivation of the catalyst (see Fig. 9). The formation of crystalline $AlVO_4$ appears to proceed by solid-state reaction between the crystalline V_2O_5 nanoparticles and the Al_2O_3 support. The interaction between vanadium and aluminum cations becomes increasingly important under reducing conditions, since reduced V^{3+} cations appear to be more compatible with the Al^{3+} cations [16]. Thus, reduced vanadia sites would interact more intensely with alumina support. The redox nature of ethane ODH reaction implies reduction–reoxidation cycles of vanadia sites. Thus, the solid-state reaction to form $AlVO_4$ during ethane ODH seems to be favored by consecutive cycles of oxidation/reduction.

The formation of $AlVO_4$ coincides with decreasing activity towards the non-selective oxidation products, CO and CO_2, but ethylene production is hardly affected (Fig. 9). This is probably due to the removal of V_2O_5 nanocrystals.

5. Conclusions

Supported vanadia catalysts consist of surface VO_x species in the sub-monolayer region (<9 V/nm^2). The surface vanadia

species become progressively polymerized with loading until monolayer surface coverage is reached. The polymeric surface VO_x species are more reducible and possess more Brønsted acid character than the isolated surface VO_x species. Comparison of the surface vanadia molecular structures with the reducibility trend demonstrated that the terminal V=O bond is not involved in the reduction rate-determining-step. The surface vanadia species coordinate to the alumina support surface and cover the exposed alumina surface Lewis acid sites. These changes in surface acidity properties, however, do not affect the activation of ethane since the ethane TOF is constant with surface vanadia coverage. This finding suggests that the bridging V–O–V bond is not critical for activation of ethane and that the catalytic active site is associated with the bridging V–O–Al bond. At low surface vanadia coverage, the exposed strong alumina Lewis acid sites are responsible for CO and CO_2 formation and the low C_2H_4 selectivity during ethane ODH. As these exposed alumina sites are progressively covered by the surface vanadia species, the vanadia-alumina system becomes more selective towards C_2H_4 formation and suppresses CO_x formation. The maximum ethylene selectivity is observed at 2.2 V/nm^2, which corresponds to ∼25% surface vanadia monolayer. The decrease in ethylene selectivity above 2.2 V/nm^2 appears to correspond with the increasing reducibility of the surface VO_x species and the presence of surface Brønsted acid sites. The crystalline V_2O_5 nanoparticles are not active for ethane conversion, but do convert ethylene to unselective CO_x. At elevated temperatures the crystalline V_2O_5 nanoparticles undergo solid-state reaction with the Al_2O_3 support to form $AlVO_4$. This solid-state reaction also suppresses the conversion of ethylene to CO_x and, consequently, enhances the ethylene selectivity.

Acknowledgements

This research was funded by CTQ2005-02802/PPQ from the Spanish Ministry of Science and Technology. The work at Lehigh University was funded by Department of Energy-Basic Energy Sciences grant DEF-G02-93ER14350.

References

[1] M.A. Bañares, Catal. Today 51 (1999) 319.
[2] J.M. López Nieto, Top. Catal. 15 (2001) 189 (and references therein).
[3] H.H. Kung, Adv. Catal. 40 (1994) 1.
[4] M.A. Bañares, M.V. Martínez-Huerta, X. Gao, J.L.G. Fierro, I.E. Wachs, Catal. Today 216 (2000) 1.
[5] I.E. Wachs, Catal. Today 100 (2005) 79.
[6] H. Tian, E.I. Ross, I.E. Wachs, J. Phys. Chem. B 110 (2006) 9593.
[7] I.E. Wachs, B.M. Weckhuysen, Appl. Catal. A Gen. 157 (1997) 67.
[8] H. Knözinger, P. Ratnasamy, Catal. Rev. Sci. Eng. 17 (1978) 31.
[9] X. Carrier, J.F. Lambert, M. Che, J. Am. Chem. Soc. 119 (1997) 10137.
[10] J.M. Kanervo, M.E. Harlin, A.O.I. Krause, M.A. Bañares, Catal. Today 78 (2003) 171.
[11] H. Tian, I.E. Wachs, L. Briand, J. Phys. Chem. B 109 (2005) 23491.
[12] M.O. Guerrero-Pérez, J.L.G. Fierro, M.A. Bañares, Top. Catal., in press.
[13] C. Morterra, G. Magnacca, Catal. Today 27 (1996) 497.
[14] H. Knözinger, Adv. Catal. 25 (1976) 184.
[15] M.A. Bañares, X. Gao, J.L.G. Fierro, I.E. Wachs, Stud. Surf. Sci. Catal. 110 (1997) 295.
[16] M. Ruitenbeek, A.J. van Dillen, F.M.F. de Groot, I.E. Wachs, J.W. Geus, D.C. Koningsberger, Top. Catal. 10 (2000) 241.
[17] M.A. Bañares, M. Martínez-Huerta, X. Gao, I.E. Wachs, J.L.G. Fierro, Stud. Surf. Sci. Catal. 130A (2000) 3125.
[18] M.A. Bañares, M.V. Martínez-Huerta, X. Gao, J.L.G. Fierro, I.E. Wachs, Catal. Today 61 (2000) 295.
[19] C.B. Wang, G. Deo, I.E. Wachs, J. Catal. 178 (1998) 640.
[20] N. Magg, B. Immaraporn, J.B. Giorgi, T. Schroeder, M. Baumer, J. Dobler, Z.L. Wu, E. Kondratenko, M. Cherian, M. Baerns, P.C. Stair, J. Sauer, H.J. Freund, J. Catal. 226 (2004) 88.
[21] M.A. Bañares, I.E. Wachs, J. Raman Spectrosc. 33 (2002) 359.
[22] B. Leyer, H. Schmelz, H. Göbel, T. Scherg, H. Knözinger, Thin Solid Films 310 (1997) 228.
[23] A. Akbas, H. Mitzel, D. Honice, React. Kinet. Catal. Lett. 59 (1996) 59.
[24] I.E. Wachs, J.-M. Jehng, G. Deo, B.M. Weckhuysen, V.V. Guliants, J.B. Benzier, Catal. Today 32 (1996) 47.